

Published in final edited form as:

*J Immunol*. 2017 January 01; 198(1): 249–256. doi:10.4049/jimmunol.1601516.

# Thymic dendritic cell subsets display distinct efficiencies and mechanisms of intercellular MHC transfer

**Charles J. Kroger**[1,*], **Nicholas A. Spidale**[1,*], **Bo Wang**[1], and **Roland Tisch**[1,2]

[1]Department of Microbiology and Immunology, University of North Carolina at Chapel Hill School of Medicine, Chapel Hill, NC 27599 USA

[2]Lineberger Comprehensive Cancer Center, University of North Carolina at Chapel Hill School of Medicine, Chapel Hill, NC 27599 USA

## Abstract

Thymic dendritic cells (DC) delete self-Ag-specific thymocytes, and drive development of FoxP3-expressing immunoregulatory T cells. Unlike medullary thymic epithelial cells (mTEC), which express and present peripheral self-Ag, DC must acquire self-Ag to mediate thymic negative selection. One such mechanism entails the transfer of surface MHC-self peptide complexes from mTEC to thymic DC. Despite the importance of thymic DC "cross-dressing" in negative selection, the factors that regulate the process, and the capacity of different thymic DC subsets to acquire MHC and stimulate thymocytes are poorly understood. Here intercellular MHC transfer by thymic DC subsets was studied using a MHC-mismatch-based *in vitro* system. Thymic conventional DC (cDC) subsets SIRPα$^+$ and CD8α$^+$ readily acquired MHC class I and II from TEC but plasmacytoid DC (pDC) were less efficient. Intercellular MHC transfer was donor cell-specific; thymic DC readily acquired MHC from TEC plus thymic or splenic DC, whereas thymic or splenic B cells were poor donors. Furthermore DC origin influenced cross-dressing; thymic versus splenic DC exhibited an increased capacity to capture TEC-derived MHC, which correlated with direct expression of EpCAM by DC. Despite similar capacities to acquire MHC-peptide complexes, thymic CD8α$^+$ cDC elicited increased T cell stimulation relative to SIRPα$^+$ cDC. DC cross-dressing was cell-contact dependent and unaffected by lipid raft disruption of donor TEC. Furthermore, blocking PI3K signaling reduced MHC acquisition by thymic CD8α$^+$ cDC and pDC but not SIRPα$^+$ cDC. These findings demonstrate that multiple parameters influence the efficiency of and distinct mechanisms drive intercellular MHC transfer by thymic DC subsets.

### Keywords

dendritic cell; epithelial cell; thymus; antigen; major histocompatibility complex

Corresponding Author: Roland Tisch; (919) 966-4766 (phone); (919) 962-8103 (fax); rmtisch@med.unc.edu.
*These authors contributed equally to this work

**AUTHOR CONTRIBUTIONS**

C.J.K. designed and performed experiments, analyzed data, and wrote the paper; N.A.S. designed and performed experiments, analyzed data, and wrote the paper; B.W. designed experiments and analyzed data; and R.T. designed experiments, analyzed data, wrote the paper, and supervised the study.

## INTRODUCTION

T cell central tolerance entails both clonal deletion of thymocytes expressing TCR with increased affinity for self-Ag, and development of Foxp3-expressing regulatory $CD4^+$ T cells ($Foxp3^+$Treg) in the medulla of the thymus. APC in the thymic medulla play an essential role in establishing T cell self-tolerance. Medullary thymic epithelial cells (mTEC) and dendritic cells (DC) are the primary APC, although B cells and macrophages are also found in the medulla. Mature mTEC express high levels of MHC class I and II, costimulatory molecules, and the transcription factor autoimmune regulator (AIRE). AIRE drives expression of multiple peripheral self-Ag which are processed and presented by mTEC (1–4). AIRE has additional functions including regulation of gene expression of various chemokines, which localize DC to the medulla (5), and facilitate interactions between mTEC and thymic DC (6). Thymic DC are broadly divided into three subsets: $CD8\alpha^+$ conventional DC (cDC), signal regulatory protein $\alpha^+$ ($SIRP\alpha^+$) cDC, and plasmacytoid DC (pDC). Noteworthy is that thymic versus peripheral DC exhibit a more mature phenotype, suggesting distinct functional properties (7). Unlike mTEC, self-Ag must be acquired by thymic DC (8–10). Thymic $CD8\alpha^+$ and $SIRP\alpha^+$ cDC localized next to blood vessels at the cortico-medullary junction capture blood borne Ag (11, 12); additionally, peripheral $SIRP\alpha^+$ cDC and pDC laden with self-Ag migrate to the thymus and contribute to central tolerance (13–15).

Thymic DC also obtain mTEC-expressed self-Ag via intercellular transfer (6, 10, 16). Self-Ag transfer is thought to expand the pool of presenting APC, and increase the efficiency of thymocyte negative selection and/or development of $Foxp3^+$Treg. The latter is particularly important since only 1–3% of mTEC express a given self-Ag (17). Engulfment of apoptotic mTEC by thymic DC is one process by which intercellular Ag transfer is achieved (10). An additional and more direct process involves intercellular transfer of plasma membrane containing MHC-peptide complexes (pMHC) from live mTEC to DC (6, 10, 16, 18). This process has been referred to as “DC cross-dressing” and is mediated by at least 2 distinct mechanisms (reviewed in (19, 20)). The first, trogocytosis or “nibbling”, entails contact-dependent, intercellular transfer of pMHC embedded in plasma membrane, and occurs between lymphocytes and innate effectors in various contexts (21–23). Uptake of pMHC containing exosomes released by donor cells is a second mechanism believed to promote DC cross-dressing (24, 25). Acquisition of donor cell-derived molecules can modify the function of the recipient cell, and in turn the nature of an immune response. Intercellular transfer of pMHC by DC was first shown to occur extrathymically, and has been associated with viral-, tumor- and alloantigen-specific T cell immunity (24, 26). In bone marrow chimera mice, donor-derived thymic DC were found to acquire pMHC from host mTEC *in vivo*, and promote thymic negative selection and $Foxp3^+$Treg development in TCR transgenic mice (27).

Despite its importance, the mechanism of intercellular MHC transfer between mTEC and thymic DC is poorly understood. A recent study reported that thymic $CD8\alpha^+$ cDC preferentially acquire MHC from mTEC *in vivo* (27). However, whether the differences reported between $CD8\alpha^+$ cDC, $SIRP\alpha^+$ cDC and pDC are due to distinct frequencies and/or spatial distribution versus intrinsic properties of a given subset are unknown. With this in

mind, we investigated intercellular pMHC transfer by thymic DC using an *in vitro* system of MHC mismatched TEC to directly test for DC subset-intrinsic properties. A hierarchy of acquisition of pMHC from live TEC and T cell stimulatory capacity was seen between thymic cDC versus pDC, and thymic versus splenic DC. Furthermore, selectivity of intercellular transfer was evident by the ability of thymic DC to acquire MHC from TEC and DC, but not B cells. Moreover, efficient MHC transfer by thymic CD8α$^+$ cDC and pDC, but not SIRPα$^+$ cDC was dependent on PI3K signaling. These findings indicate that intercellular transfer of MHC by thymic DC is a complex process that is influenced by a number of parameters.

## MATERIALS AND METHODS

### Mice

NOD/LtJ (NOD), BALB/cJ (BALB/c), NOD.Cg-Tg(TcraBDC2.5, TcrbBDC2.5)1Doi/DoiJ x NOD.129P2(C)-*Tcra*$^{tm1Mjo}$/DoiJ (BDC2.5), C57BL/6J (B6) and NOD.129S2(B6)-*Aire*$^{tm1.1Doi}$/DoiJ (NOD.AIRE$^{-/-}$) were purchased from the Jackson Laboratories and housed under specific pathogen-free conditions. Both male and female mice 6–8 wks of age were used but sex-matched within an experiment. No differences between cells isolated from male or female mice were observed for any assay. All animal procedures were approved by the Institutional Animal Care and Use Committee at the University of North Carolina at Chapel Hill.

### Cell isolation

For “bulk” DC isolation, thymi or spleens were harvested, minced and digested for 30 min at room temperature with 1 mg/ml collagenase D and 20 μg/ml DNAse I (Roche) in R2 medium (RPMI 1640, 2% FCS, 10 mM HEPES pH 7.4). Following a 5 min incubation with 10 mM EDTA, cells were centrifuged through an OptiPrep Axis-Shield gradient (28), and DC purified with CD11c microbeads and an AutoMACS separator (Miltenyi Biotec).

To isolate TEC, thymi were digested with 1 mg/ml collagenase D and 20 μg/ml DNAse I in R2 at 37°C (3 rounds, 15 min each), 15 min with 1.25 mg/ml collagenase/Dispase (Roche) and DNAse I, and 5 min with 10 mM EDTA. Cells were centrifuged through a Percoll (GE Healthcare) gradient, and TEC purified via CD45$^+$ cell depletion on an AutoMACS separator.

Thymic B and splenic B cells (B220$^+$CD11c$^-$) were FACS sorted or enriched using EasySep Mouse B Cell Isolation Kit (Stem Cell Technologies). BDC2.5 CD4$^+$ T cells were isolated with a CD4$^+$ T cell isolation kit II (Miltenyi Biotec).

### Flow Cytometry

The following mAb were purchased from BD Biosciences, BioLegend, eBioscience, Life Technologies, and Cell Signaling Technology: αCD11c (N418), αCD8α (53-6.7), αSIRPα (P84), αCD45RA (14.8), αB220 (RA3-6B2), αCD3ε (145-2C11), αCD49b (DX5), αCD19 (1D3), αerythroid cells (Ter-119), αIA$^{k/g7}$ (10-3.6), αIE$^d$ (14-4-4S), αIA$^b$ (KH74), αH2D$^d$ (34-2-12), αepithelial cell adhesion molecule (EpCAM, G8.8), αCD45.1 (A20), αCD45.2

(104), and αphosphorylated (p) $AKT_{Thr308}$ (D25E6). To label lipid rafts, TEC or B cells were incubated with 1 μg/ml cholera toxin B subunit*Alexa Fluor 647 (CTxB, Life Technologies) in PBS for 15–30 min, then washed. Cells were Fc receptor blocked using 2.4G2 mAb prior to staining. Dead cells were excluded using propidium iodide, DAPI, 7AAD, or LIVE/DEAD dye (Life Technologies). Data were acquired on an LSR II, LSRFortessa (BD Biosciences) or CyAN ADP (Beckman Coulter) and analyzed using FlowJo (TreeStar Inc.). Sorting of DC subsets was performed on a MoFlo XDP (Beckman Coulter) or FACSAria III (BD Biosciences) to a purity >95%. To analyze proliferation, purified BDC2.5 $CD4^+$ T cells were labeled with 5 μM CellTrace Violet (CTV; Life Technologies).

### Intercellular MHC Transfer Assay

To examine intercellular MHC transfer *in vitro*, cells were isolated from MHC-mismatched NOD ($H2^{g7}$), BALB/c ($H2^d$) or B6 ($H2^b$) mice. DC, and MHC "donor" TEC, DC, or B cells were co-cultured for 2–4 h in R10 (RPMI 1640/10% FCS, 4 mM L-glutamine, 1x non-essential amino acids, 1 mM sodium pyruvate, 100 units/ml penicillin, 100 μg/ml streptomycin, 55 μM β-mercaptoethanol, 10 mM HEPES pH7.4) and analyzed via flow cytometry. In some experiments, a 0.4 μm TransWell apparatus (Corning) was used. For inhibition of PI3K, DC were pretreated with LY294002 (LY29, Cell Signaling) for 30–60 min prior to the addition of TEC and during the co-culture. To examine $pAKT_{Thr308}$ levels, NOD DC were cultured with B6 TEC, and then fixed and permeabilized according to the manufacturer's directions. Lipid raft disruption experiments were performed in Opti-MEM (Life Technologies) + 5% delipidized FCS (Gemini Bio-Products). TEC were treated with methyl β-cyclodextrin (MβCD) or Nystatin (Sigma-Aldrich) for 15 or 60 min, respectively, washed, and cultured with DC as above.

### Quantitative RT-PCR

Thymic DC were FACS sorted, RNA isolated using TriZol (Life Technologies), and cDNA synthesized using Maxima H Minus Reverse Transcriptase (Thermo Scientific) with an $oligo(dT)_{18}$ primer. qPCR was performed using the Maxima SYBR Green Master Mix (Thermo Scientific) and a MyIQ iCycler (Bio-Rad). Cycling conditions consisted of: 95°C, 10 min and 40 cycles of 95°C, 15 s; 60°C, 30 s; 72°C, 30 s followed by dissociation curve analysis. Relative expression of *Epcam* was assessed by the comparative Ct (ΔΔCt) method (29) using *Hprt* as the endogenous reference and $EpCAM^-$ cDC as the calibrator sample. The following primers were synthesized by the UNC-CH Nucleic Acids Core Facility for qPCR: *Epcam* Forward, 5′–GCGGCTCAGAGAGACTGTG–3′; *Epcam* Reverse, 5′–CCAAGCATTTAGACGCCAGTTT–3′; *Hprt* Forward, 5′–GCTATAAATTCTTTGCTGACCTGCTG–3′; *Hprt* Reverse, 5′–AATTACTTTTATGTCCCCTGTTGACTGG–3′.

## RESULTS

### Thymic DC acquire MHC class I and II from TEC and DC but not B cells

To study in detail intercellular MHC class I and II transfer and test for thymic DC subset-specific properties, an *in vitro* co-culture system relying on MHC-mismatched cells was

employed (Fig. 1A). NOD ($H2^{g7}$) thymic DC were tested for the capacity to capture $IE^d$ and $H2D^d$ from various types of BALB/c ($H2^d$) APC including TEC, as well as DC and B cells from the thymus and spleen. The gating strategy to identify the respective thymic DC subsets is depicted in Supplemental Fig. 1. Co-culture with BALB/c TEC resulted in up to 60% of NOD thymic DC rapidly acquiring MHC (e.g. within 4 h) (Fig. 1B,E). $CD8\alpha^+$ and $SIRP\alpha^+$ DC exhibited a similar frequency of $IE^{d+}$ (~60%) and $H2D^{d+}$ (~45%) cells (Fig. 1B,E). On the other hand, pDC displayed reduced MHC acquisition with ~20% and ~10% staining for $IE^d$ and $H2D^d$, respectively (Fig. 1B,E).

A similar pattern of acquisition was observed when BALB/c thymic and splenic DC were used as MHC donors, although MHC transfer with splenic DC was less efficient (Fig. 1C,E). A trend towards preferential acquisition of MHC class II versus class I from BALB/c thymic and splenic DC was observed (Fig. 1C,E), which likely reflected the increased level of $IE^d$ versus $H2D^d$ by the respective donor cells (Fig. 1F). Strikingly, when BALB/c thymic or splenic B cells were tested as MHC donors (Fig. 1F), no significant transfer of $IE^d$ or $H2D^d$ to NOD thymic DC was observed (Fig. 1D,E). Similarly, only a minimal increase (<8%) in $IE^{d+}$ NOD thymic DC was detected when BALB/c splenic B cells were activated prior by αIgM, αCD40 or LPS, and surface expression of $IE^d$ increased >5-fold (Supplemental Fig. 2). Analogous results were obtained when BALB/c thymic DC were assessed for MHC acquisition from NOD donor cells (data not shown). These data demonstrate that: i) thymic $CD8\alpha^+$ and $SIRP\alpha^+$ cDC but not pDC efficiently acquire MHC class I and II, and ii) intercellular MHC transfer is readily achieved with donor TEC, and thymic and splenic DC, but not B cells from the thymus and spleen.

## Thymic versus splenic DC exhibit enhanced acquisition of TEC MHC, which correlates with EpCAM expression

Thymic DC display a more activated phenotype relative to splenic DC (7). With this in mind, we tested if differences existed between thymic and splenic NOD DC to acquire MHC. The frequency of $IE^{d+}$ and $H2D^{b+}$ $CD8\alpha^+$ cDC was slightly increased for thymic versus splenic DC, whereas a greater difference was seen among $SIRP\alpha^+$ cDC (Fig. 2A–E). However, thymic $SIRP\alpha^+$ and $CD8\alpha^+$ cDC acquired significantly more (up to 2–3-fold) $IE^d$ and $H2D^d$ based on MFI, compared to the corresponding splenic cDC subsets (Fig. 2C,E).

Analyses identified EpCAM as a key marker reflecting the efficiency of MHC acquisition between thymic and splenic DC, as well among the thymic cDC subsets. Both the frequency (up to 7-fold) and MFI (up to 10-fold) of EpCAM expression were elevated for the respective thymic cDC subsets (Fig. 2F,G). pDC exhibited both a reduced frequency of $EpCAM^+$ thymic (and splenic) cells, as well as the MFI of EpCAM compared to cDC (Fig. 2F,G). Notably, the level of acquired MHC was significantly increased for $EpCAM^+$ thymic $SIRP\alpha^+$ and $CD8\alpha^+$ cDC relative to the corresponding $EpCAM^-$ thymic cDC subsets (Fig. 2H).

Earlier work reported that thymic DC acquire EpCAM upon capturing plasma membrane from $EpCAM^+$ mTEC (10). Our findings, however, suggested that thymic (and splenic) DC actually expressed EpCAM. To confirm this observation, thymic cDC were FACS-sorted into $EpCAM^+$ and $EpCAM^-$ populations (Fig. 2I) and *Epcam* mRNA measured via qRT-

PCR. EpCAM$^+$ cDC expressed ~70-fold more *Epcam* mRNA compared to EpCAM$^-$ cDC (Fig. 2J). By comparison, TEC expressed ~3-fold more *Epcam* mRNA than EpCAM$^+$ cDC (Fig. 2J). Together these results demonstrate that acquisition of MHC class I and II from TEC is not unique to steady-state thymic DC, although thymic DC are more efficient than splenic DC at MHC capture, which in turn correlates with increased EpCAM expression.

## A hierarchy exists among cross-dressing thymic DC subsets to stimulate T cells

A key question was whether cross-dressing thymic DC were capable of stimulating T cells specific for the transferred pMHC. Isolated NOD TEC were pulsed with the IA$^{g7}$-restricted sBDC mimetic peptide, and co-cultured with BALB/c thymic DC. The total thymic DC population was then FACS sorted (Fig. 3A) and tested for stimulation of CTV-labeled, TCR transgenic BDC2.5 CD4$^+$ T cells specific for sBDC (Fig. 3B). As expected, robust BDC2.5 CD4$^+$ T cell proliferation was observed when peptide-pulsed live TEC were directly used as APC at a 1:10 TEC to T cell ratio (Fig. 3B). Importantly, sorted DC after co-culture with TEC also induced BDC2.5 CD4$^+$ T cell proliferation at a 1:2 DC to T cell ratio, that was dependent on the sBDC concentration used to pulse donor TEC (Fig. 3B,C). Therefore the cross-dressed DC present functional TEC derived MHC molecules that efficiently induce the activation of T cells.

Next, whether the 3 thymic DC subsets exhibited distinct stimulatory capacities following cross-dressing was examined. FACS-sorted pDC induced only minimal BDC2.5 CD4$^+$ T cell proliferation (Fig. 3D). In contrast, robust of BDC2.5 CD4$^+$ T cell proliferation was stimulated by FACS-sorted SIRPα$^+$ and CD8α$^+$ cDC (Fig. 3D). Interestingly, CD8α$^+$ cDC were the most potent activators of BDC2.5 CD4$^+$ T cells at both the low and high sBDC concentration, promoting increased proliferation compared to SIRPα$^+$ cDC (Fig. 3D). BALB/c thymic CD8α$^+$ versus SIRPα$^+$ cDC expressed similar levels of CD80, CD86, and CD40 (data not shown), which indicated that differences in proliferation were independent of co-stimulatory molecules. Together, these data demonstrate that acquired pMHC effectively stimulate T cells, and that a hierarchy for CD4$^+$ T cell stimulation exists among the subsets of cross-dressing thymic DC.

## MHC transfer requires TEC and thymic DC contact and is independent of lipid raft integrity of donor cells

The factors that regulate intercellular MHC transfer between TEC and thymic DC have not been determined. Initially, we investigated whether the efficiency of MHC transfer is influenced by donor cell lipid rafts, in which MHC class II are preferentially found (30). Lipid rafts of BALB/c donor cells were labeled with fluorochrome-conjugated CTxB, and MHC acquisition by NOD thymic DC measured. Efficient transfer of both TEC-derived IE$^d$ and CTxB-labeled lipid rafts to the respective thymic DC subsets was observed (Fig. 4A). Interestingly, although MHC acquisition from splenic B cells was limited, lipid raft transfer was not; specifically the majority of thymic DC stained positively for CTxB-labeled lipid rafts (Fig. 4B), indicating efficient yet restrictive plasma membrane exchange between DC and B cells.

To determine whether TEC lipid raft integrity of donor TEC was necessary for MHC capture by thymic DC, lipid rafts were disrupted in BALB/c TEC by MβCD, which removes cell membrane cholesterol. No difference in thymic DC acquisition of $IE^d$ was seen between untreated or MβCD-treated donor TEC (Fig. 4C). Similar results were observed utilizing nystatin, which disrupts lipid raft integrity by sequestering cholesterol within the cell membrane (Supplemental Fig. 3).

Intercellular transfer of MHC is mediated by either cell contact-dependent trogocytosis or uptake of exosomes released by donor cells (20). To distinguish between these 2 mechanisms, BALB/c TEC labeled with CTxB and NOD thymic $SIRP\alpha^+$ and $CD8\alpha^+$ cDC were cultured using a transwell apparatus. Consistent with above results (Fig. 1B,E) ~50% of $SIRP\alpha^+$ and $CD8\alpha^+$ cDC acquired $IE^d$ upon direct culture with donor TEC (Fig. 4D, middle panels). In contrast, no acquisition of $IE^d$ and an ~85% MFI reduction in CTxB transfer was observed when thymic $SIRP\alpha^+$ and $CD8\alpha^+$ cDC were separated from TEC (Fig. 4D, lower panels). Collectively, these results indicate that thymic DC via cell contact efficiently acquire MHC and lipid rafts, and that lipid raft integrity of donor TEC is not required for efficient intercellular MHC transfer.

### Efficiency of MHC acquisition by pDC and $CD8\alpha^+$ cDC but not $SIRP\alpha^+$ cDC is reduced by blocking PI3K signaling

Since T cells require PI3K signaling during TCR-mediated trogocytosis (23), we hypothesized that this pathway also regulates MHC acquisition by thymic DC. Accordingly, phosphorylation of AKT, a conical intermediate in the PI3K signaling pathway was studied. NOD thymic DC were co-cultured with B6 TEC, and levels of $pAKT_{Thr308}$ measured by flow cytometry. $IA^{b+}$ pDC, and to a lesser extent $IA^{b+}$ $CD8\alpha^+$ cDC exhibited elevated levels of $pAKT_{Thr308}$ compared to $IA^{b-}$ pDC and $CD8\alpha^+$ cDC, respectively (Fig. 5A,B). In contrast, a minimal increase in the level of $pAKT_{Thr308}$ was detected between $IA^{b+}$ versus $IA^{b-}$ $SIRP\alpha^+$ cDC (Fig. 5A,B). Constitutive levels of $pAKT_{Thr308}$, however, were markedly greater in $SIRP\alpha^+$ cDC than that detected in both pDC and $CD8\alpha^+$ cDC (Fig. 5A).

The above findings suggested that PI3K signaling was involved in MHC acquisition by thymic pDC and $CD8\alpha^+$ cDC but not $SIRP\alpha^+$ cDC. To test this scenario, NOD thymic DC were pretreated with the PI3K inhibitor LY29 and the efficiency of $IE^d$ transfer from BALB/c TEC measured. The frequency of $IE^{d+}$ $SIRP\alpha^+$ cDC as well as the MFI of captured $IE^d$ was not significantly affected at the doses of LY29 tested (Fig. 5C–E). In contrast, both the frequency of $IE^{d+}$ cells and the level of acquired MHC class II by pDC and $CD8\alpha^+$ cDC were significantly reduced by LY29 treatment (Fig. 5B–D); notably DC viability was minimally affected by the different LY29 concentrations tested (data not shown). In sum, these results demonstrate that PI3K signaling is necessary for efficient MHC acquisition by pDC and $CD8\alpha^+$ cDC, and that $SIRP\alpha^+$ cDC cross-dressing is regulated in a distinct manner.

## DISCUSSION

Unidirectional transfer of pMHC between mTEC and thymic DC has been reported *in vivo*, and shown to impact thymic negative selection and $Foxp3^+$Treg development (10). The

parameters that influence thymic intercellular pMHC transfer, and the acquisition capabilities of the respective thymic DC subsets, however, are poorly defined. This study provides novel insight into these key issues, demonstrating that: i) thymic DC subsets differ in the capacity to acquire MHC and stimulate T cells, ii) the identity of the donor cell type influences the efficiency of MHC acquisition by thymic DC, iii) thymic versus splenic DC exhibit an enhanced capacity to capture MHC, and iv) distinct mechanisms are utilized for MHC acquisition by the thymic DC subsets.

A hierarchy in the efficiency of intercellular MHC transfer was found among thymic DC subsets and the corresponding splenic DC subsets. Acquisition of MHC class I and II was more efficient for: i) thymic SIRPα$^+$ and CD8α$^+$ cDC compared to thymic pDC (Fig. 1), and ii) thymic versus splenic cDC (Fig. 2). Thymic CD8α$^+$ and SIRPα$^+$ cDC acquired MHC to the same extent which is in contrast with an earlier study showing preferential acquisition by CD8α$^+$ cDC *in vivo* (27). The ~3-fold increase in the frequency of CD8α$^+$ cDC in the adult mouse thymus (Supplemental Fig. 1), however, would be expected to aid MHC uptake versus SIRPα$^+$ cDC. Notably, increased EpCAM expression correlated with enhanced efficiency of MHC acquisition by the respective DC (Fig. 2). EpCAM has been used as a marker for intercellular MHC transfer between DC and EpCAM$^+$ mTEC or tumor cells *in vivo* (10, 31). Our data demonstrate that in addition to capturing EpCAM, thymic DC directly express this glycoprotein, with RNA levels only ~3-fold less than TEC (Fig. 2). Consistent with this finding, surface EpCAM is detected on DC in peripheral lymphoid organs, such as skin-draining lymph nodes and the spleen (32), neither of which possess large numbers of potential donor EpCAM$^+$ stromal cells (33). EpCAM mediates homophilic adhesion (34), and therefore may enhance the interaction between EpCAM$^+$ thymic DC and mTEC (or other EpCAM$^+$ DC). Indeed, trogocytosis is generally considered to be receptor-mediated, and thymic DC have been found tethered to TEC *in vivo* (35). It is intriguing that thymic B cells, of which <5% express EpCAM (data not shown), function as poor MHC donors (Fig. 1,4). A direct role for EpCAM facilitating and/or enhancing an interaction and subsequent MHC transfer between mTEC and thymic DC still needs to be determined. Notably, ectopic expression of EpCAM by an epithelial thymic cell line induced cytoskeletal and membrane reorganization leading to active membrane exchange (36). Other molecules also likely contribute to DC cross-dressing; for instance despite a similar capacity to acquire MHC, SIRPα$^+$ cDC express ~2-fold more surface EpCAM than CD8α$^+$ cDC (Fig. 2), and EpCAM$^-$ thymic DC continue to acquire MHC albeit less efficiently (Fig. 2). MHC acquisition by thymic DC, however, was unaffected by Ab blockade of the class A scavenger receptor (data not shown), which has been reported to promote intercellular transfer by non-human primate monocyte-derived DC (37).

Interestingly, recent work by Ardouin *et al.* demonstrated that the maturation status of thymic CD8α$^+$ (XCR1$^+$) cDC impacts the efficacy of cross-presentation of TEC-derived self-Ag (38). Here, mature (CCR7$^+$) but not immature (CCR7$^-$) thymic CD8α$^+$ cDC cross-present a neo-self Ag expressed by TEC (38). In support of this observation, we have found that EpCAM expression was increased among mature CCR7$^+$ (>40%) versus immature CCR7$^-$ (<20%) CD8α$^+$ (XCR1$^+$) cDC residing in the thymus of NOD and B6 mice (data not shown). Furthermore, thymic versus splenic CD8α$^+$ and SIRPα$^+$ cDC exhibit a more "mature" phenotype which is coupled with increased EpCAM expression and a superior

cross-dressing ability (Fig. 2). Variation in maturation and corresponding gene expression profiles may further impact other aspects of thymic DC cross-dressing, such as the role of PI3K.

A hierarchy in T cell stimulation was also detected among cross-dressing thymic DC subsets. Thymic cDC exhibited a greater T cell stimulatory capacity compared to pDC (Fig. 3). The latter is consistent with reduced MHC acquisition by thymic pDC (Figs. 1,5) *in vitro* and *in vivo* (27). Cross-dressing thymic CD8α$^+$ cDC exhibited enhanced CD4$^+$ T cell stimulation relative to thymic SIRPα$^+$ cDC, despite similar pMHC acquisition, and expression of costimulatory molecules. Differences in turnover or stability of acquired pMHC may contribute to the increased stimulatory capacity of cross-dressing CD8α$^+$ cDC. Thymic CD8α$^+$ cDC acquiring pMHC from mTEC *in vivo* were found to play a key role in the development of Foxp3$^+$Treg specific for Aire-dependent Ag (39). An enhanced stimulatory function coupled with an increased frequency may favor cross-dressing thymic CD8α$^+$ over SIRPα$^+$ cDC, particularly when specific pMHC are expected to be limiting *in vivo*.

Our findings demonstrate that intercellular MHC transfer is rapid, and requires direct contact between TEC and thymic DC (Fig. 4), consistent with the process of trogocytosis. However, cell contact alone was insufficient for MHC capture, and that the identity of donor cell was critical. Intercellular MHC transfer was readily detected for donor mTEC, less so for DC, but not seen for thymic or splenic B cells (Fig. 1). B cell activation and upregulation of surface MHC expression only minimally increased DC cross-dressing (Supplemental Fig. 2). Despite the lack of MHC transfer, lipid rafts from B cells were efficiently captured by thymic DC in a cell contact manner (Fig. 4), indicating efficient plasma membrane exchange. The latter suggests an element of selectivity in MHC acquisition by thymic DC. These findings also suggest that thymic B cells contribute to negative selection (40) by directly functioning as APC and not by “donating” pMHC. Disrupting lipid rafts in donor cells had no effect on MHC acquisition by thymic DC (Fig. 4), indicating that lipid rafts do not “mark” MHC for capture. Whether the efficiency and/or selectivity of intercellular MHC transfer are driven by similar or distinct receptor-ligand interactions (e.g. EpCAM-mediated) is a possibility being investigated.

A key observation made in our study is that PI3K signaling was necessary for efficient MHC acquisition by thymic DC (Fig. 5). A similar result has been reported for T cells and TCR-mediated trogocytosis (23). The requirement for PI3K signaling, however, was dependent on thymic DC subset. Induced $pAKT_{Thr308}$ levels were detected in thymic pDC and CD8α$^+$ cDC following MHC acquisition, which in turn was significantly reduced by inhibiting PI3K signaling (Fig. 5). How PI3K signaling is activated and regulates MHC acquisition by thymic pDC and CD8α$^+$ cDC needs to be further investigated. Also of keen interest is the nature of the signaling event(s) regulating MHC acquisition by thymic SIRPα$^+$ cDC. One possible scenario is that constitutively high PI3K signaling, reflected by elevated $pAKT_{Thr308}$ levels (Fig. 5), “primes” SIRPα$^+$ cDC for efficient MHC capture. On the other hand, due to comparatively low basal levels of $pAKT_{Thr308}$, PI3K signaling must be elevated to achieve a given threshold needed for efficient MHC acquisition in thymic pDC and CD8α$^+$ cDC. Alternatively, regulation of MHC acquisition by thymic SIRPα$^+$ cDC may be

PI3K-independent suggesting that a distinct receptor may contribute to the cross-dressing process.

In summary, this study provides evidence that intercellular MHC transfer by thymic DC is complex and influenced by a variety of parameters. Our *in vitro* model system can be exploited to further define the mechanisms by which thymic DC acquire MHC and other proteins, and in turn refine our understanding of the relative role of DC in central tolerance.

## Supplementary Material

Refer to Web version on PubMed Central for supplementary material.

## Acknowledgments

This study was supported by funding from the National Institutes of Health to R.T. (1R01AI083269). N.A.S. and C.J.K. were supported by a National Institutes of Health Training Grant (T32 AI007273). The UNC Flow Cytometry Core Facility is supported in part by P30 CA016086 Cancer Center Core Support Grant to the UNC Lineberger Comprehensive Cancer Center, and North Carolina Biotech Center Institutional Support Grant 2005-IDG-1016.

## Abbreviations

| | |
|---|---|
| **cDC** | conventional DC |
| **cTEC** | cortical TEC |
| **CTxB** | cholera toxin B subunit |
| **DC** | dendritic cell |
| **mTEC** | medullary TEC |
| **pDC** | plasmacytoid DC |
| **SIRPα** | signal regulatory protein alpha |
| **TEC** | thymic epithelial cell |

## References

1. Anderson MS, Venanzi ES, Klein L, Chen Z, Berzins SP, Turley SJ, von Boehmer H, Bronson R, Dierich A, Benoist C, Mathis D. Projection of an immunological self shadow within the thymus by the aire protein. Science. 2002; 298:1395–1401. [PubMed: 12376594]
2. Derbinski J, Schulte A, Kyewski B, Klein L. Promiscuous gene expression in medullary thymic epithelial cells mirrors the peripheral self. Nat Immunol. 2001; 2:1032–1039. [PubMed: 11600886]
3. Hinterberger M, Aichinger M, Prazeres da Costa O, Voehringer D, Hoffmann R, Klein L. Autonomous role of medullary thymic epithelial cells in central CD4(+) T cell tolerance. Nat Immunol. 2010; 11:512–519. [PubMed: 20431619]
4. Klein L, Hinterberger M, von Rohrscheidt J, Aichinger M. Autonomous versus dendritic cell-dependent contributions of medullary thymic epithelial cells to central tolerance. Trends Immunol. 2011; 32:188–193. [PubMed: 21493141]
5. Lei Y, Ripen AM, Ishimaru N, Ohigashi I, Nagasawa T, Jeker LT, Bosl MR, Hollander GA, Hayashi Y, de Malefyt WR, Nitta T, Takahama Y. Aire-dependent production of XCL1 mediates medullary

accumulation of thymic dendritic cells and contributes to regulatory T cell development. J Exp Med. 2011; 208:383–394. [PubMed: 21300913]

6. Hubert FX, Kinkel SA, Davey GM, Phipson B, Mueller SN, Liston A, Proietto AI, Cannon PZ, Forehan S, Smyth GK, Wu L, Goodnow CC, Carbone FR, Scott HS, Heath WR. Aire regulates the transfer of antigen from mTECs to dendritic cells for induction of thymic tolerance. Blood. 2011; 118:2462–2472. [PubMed: 21505196]
7. Spidale NA, Wang B, Tisch R. Cutting edge: Antigen-specific thymocyte feedback regulates homeostatic thymic conventional dendritic cell maturation. J Immunol. 2014; 193:21–25. [PubMed: 24890722]
8. Liston A, Lesage S, Wilson J, Peltonen L, Goodnow CC. Aire regulates negative selection of organ-specific T cells. Nat Immunol. 2003; 4:350–354. [PubMed: 12612579]
9. Hubert FX, Kinkel SA, Webster KE, Cannon P, Crewther PE, Proeitto AI, Wu L, Heath WR, Scott HS. A specific anti-Aire antibody reveals aire expression is restricted to medullary thymic epithelial cells and not expressed in periphery. J Immunol. 2008; 180:3824–3832. [PubMed: 18322189]
10. Koble C, Kyewski B. The thymic medulla: a unique microenvironment for intercellular self-antigen transfer. J Exp Med. 2009; 206:1505–1513. [PubMed: 19564355]
11. Atibalentja DF, Byersdorfer CA, Unanue ER. Thymus-blood protein interactions are highly effective in negative selection and regulatory T cell induction. J Immunol. 2009; 183:7909–7918. [PubMed: 19933868]
12. Atibalentja DF, Murphy KM, Unanue ER. Functional redundancy between thymic CD8alpha+ and Sirpalpha+ conventional dendritic cells in presentation of blood-derived lysozyme by MHC class II proteins. J Immunol. 2011; 186:1421–1431. [PubMed: 21178002]
13. Li J, Park J, Foss D, Goldschneider I. Thymus-homing peripheral dendritic cells constitute two of the three major subsets of dendritic cells in the steady-state thymus. J Exp Med. 2009; 206:607–622. [PubMed: 19273629]
14. Bonasio R, Scimone ML, Schaerli P, Grabie N, Lichtman AH, von Andrian UH. Clonal deletion of thymocytes by circulating dendritic cells homing to the thymus. Nat Immunol. 2006; 7:1092–1100. [PubMed: 16951687]
15. Hadeiba H, Lahl K, Edalati A, Oderup C, Habtezion A, Pachynski R, Nguyen L, Ghodsi A, Adler S, Butcher EC. Plasmacytoid dendritic cells transport peripheral antigens to the thymus to promote central tolerance. Immunity. 2012; 36:438–450. [PubMed: 22444632]
16. Millet V, Naquet P, Guinamard RR. Intercellular MHC transfer between thymic epithelial and dendritic cells. Eur J Immunol. 2008; 38:1257–1263. [PubMed: 18412162]
17. Derbinski J, Pinto S, Rosch S, Hexel K, Kyewski B. Promiscuous gene expression patterns in single medullary thymic epithelial cells argue for a stochastic mechanism. Proc Natl Acad Sci U S A. 2008; 105:657–662. [PubMed: 18180458]
18. Gallegos AM, Bevan MJ. Central tolerance to tissue-specific antigens mediated by direct and indirect antigen presentation. J Exp Med. 2004; 200:1039–1049. [PubMed: 15492126]
19. Thery C, Ostrowski M, Segura E. Membrane vesicles as conveyors of immune responses. Nat Rev Immunol. 2009; 9:581–593. [PubMed: 19498381]
20. Nakayama M. Antigen Presentation by MHC-Dressed Cells. Front Immunol. 2014; 5:672. [PubMed: 25601867]
21. Hwang I, Huang JF, Kishimoto H, Brunmark A, Peterson PA, Jackson MR, Surh CD, Cai Z, Sprent J. T cells can use either T cell receptor or CD28 receptors to absorb and internalize cell surface molecules derived from antigen-presenting cells. J Exp Med. 2000; 191:1137–1148. [PubMed: 10748232]
22. Hudrisier D, Aucher A, Puaux AL, Bordier C, Joly E. Capture of target cell membrane components via trogocytosis is triggered by a selected set of surface molecules on T or B cells. J Immunol. 2007; 178:3637–3647. [PubMed: 17339461]
23. Martinez-Martin N, Fernandez-Arenas E, Cemerski S, Delgado P, Turner M, Heuser J, Irvine DJ, Huang B, Bustelo XR, Shaw A, Alarcon B. T cell receptor internalization from the immunological synapse is mediated by TC21 and RhoG GTPase-dependent phagocytosis. Immunity. 2011; 35:208–222. [PubMed: 21820331]

24. Wakim LM, Bevan MJ. Cross-dressed dendritic cells drive memory CD8+ T-cell activation after viral infection. Nature. 2011; 471:629–632. [PubMed: 21455179]
25. Thery C, Duban L, Segura E, Veron P, Lantz O, Amigorena S. Indirect activation of naive CD4+ T cells by dendritic cell-derived exosomes. Nat Immunol. 2002; 3:1156–1162. [PubMed: 12426563]
26. Dolan BP, Gibbs KD Jr, Ostrand-Rosenberg S. Dendritic cells cross-dressed with peptide MHC class I complexes prime CD8+ T cells. J Immunol. 2006; 177:6018–6024. [PubMed: 17056526]
27. Perry JS, Lio CW, Kau AL, Nutsch K, Yang Z, Gordon JI, Murphy KM, Hsieh CS. Distinct contributions of Aire and antigen-presenting-cell subsets to the generation of self-tolerance in the thymus. Immunity. 2014; 41:414–426. [PubMed: 25220213]
28. Ruedl C, Rieser C, Bock G, Wick G, Wolf H. Phenotypic and functional characterization of CD11c + dendritic cell population in mouse Peyer's patches. Eur J Immunol. 1996; 26:1801–1806. [PubMed: 8765024]
29. Schmittgen TD, Livak KJ. Analyzing real-time PCR data by the comparative C(T) method. Nat Protoc. 2008; 3:1101–1108. [PubMed: 18546601]
30. Anderson HA, Hiltbold EM, Roche PA. Concentration of MHC class II molecules in lipid rafts facilitates antigen presentation. Nat Immunol. 2000; 1:156–162. [PubMed: 11248809]
31. Bonaccorsi I, Morandi B, Antsiferova O, Costa G, Oliveri D, Conte R, Pezzino G, Vermiglio G, Anastasi GP, Navarra G, Munz C, Di Carlo E, Mingari MC, Ferlazzo G. Membrane transfer from tumor cells overcomes deficient phagocytic ability of plasmacytoid dendritic cells for the acquisition and presentation of tumor antigens. J Immunol. 2014; 192:824–832. [PubMed: 24337377]
32. Borkowski TA, Nelson AJ, Farr AG, Udey MC. Expression of gp40, the murine homologue of human epithelial cell adhesion molecule (Ep-CAM), by murine dendritic cells. Eur J Immunol. 1996; 26:110–114. [PubMed: 8566052]
33. Fletcher AL, Lukacs-Kornek V, Reynoso ED, Pinner SE, Bellemare-Pelletier A, Curry MS, Collier AR, Boyd RL, Turley SJ. Lymph node fibroblastic reticular cells directly present peripheral tissue antigen under steady-state and inflammatory conditions. J Exp Med. 2010; 207:689–697. [PubMed: 20308362]
34. Litvinov SV, Velders MP, Bakker HA, Fleuren GJ, Warnaar SO. Ep-CAM: a human epithelial antigen is a homophilic cell-cell adhesion molecule. J Cell Biol. 1994; 125:437–446. [PubMed: 8163559]
35. Sanos SL, Nowak J, Fallet M, Bajenoff M. Stromal cell networks regulate thymocyte migration and dendritic cell behavior in the thymus. J Immunol. 2011; 186:2835–2841. [PubMed: 21278345]
36. Maghzal N, Vogt E, Reintsch W, Fraser JS, Fagotto F. The tumor-associated EpCAM regulates morphogenetic movements through intracellular signaling. J Cell Biol. 2010; 191:645–659. [PubMed: 20974811]
37. Harshyne LA, Zimmer MI, Watkins SC, Barratt-Boyes SM. A role for class A scavenger receptor in dendritic cell nibbling from live cells. J Immunol. 2003; 170:2302–2309. [PubMed: 12594251]
38. Ardouin L, Luche H, Chelbi R, Carpentier S, Shawket A, Montanana Sanchis F, Santa Maria C, Grenot P, Alexandre Y, Gregoire C, Fries A, Vu Manh TP, Tamoutounour S, Crozat K, Tomasello E, Jorquera A, Fossum E, Bogen B, Azukizawa H, Bajenoff M, Henri S, Dalod M, Malissen B. Broad and Largely Concordant Molecular Changes Characterize Tolerogenic and Immunogenic Dendritic Cell Maturation in Thymus and Periphery. Immunity. 2016; 45:305–318. [PubMed: 27533013]
39. Lin J, Yang L, Silva HM, Trzeciak A, Choi Y, Schwab SR, Dustin ML, Lafaille JJ. Increased generation of Foxp3(+) regulatory T cells by manipulating antigen presentation in the thymus. Nat Commun. 2016; 7:10562. [PubMed: 26923114]
40. Yamano T, Nedjic J, Hinterberger M, Steinert M, Koser S, Pinto S, Gerdes N, Lutgens E, Ishimaru N, Busslinger M, Brors B, Kyewski B, Klein L. Thymic B Cells Are Licensed to Present Self Antigens for Central T Cell Tolerance Induction. Immunity. 2015; 42:1048–1061. [PubMed: 26070482]

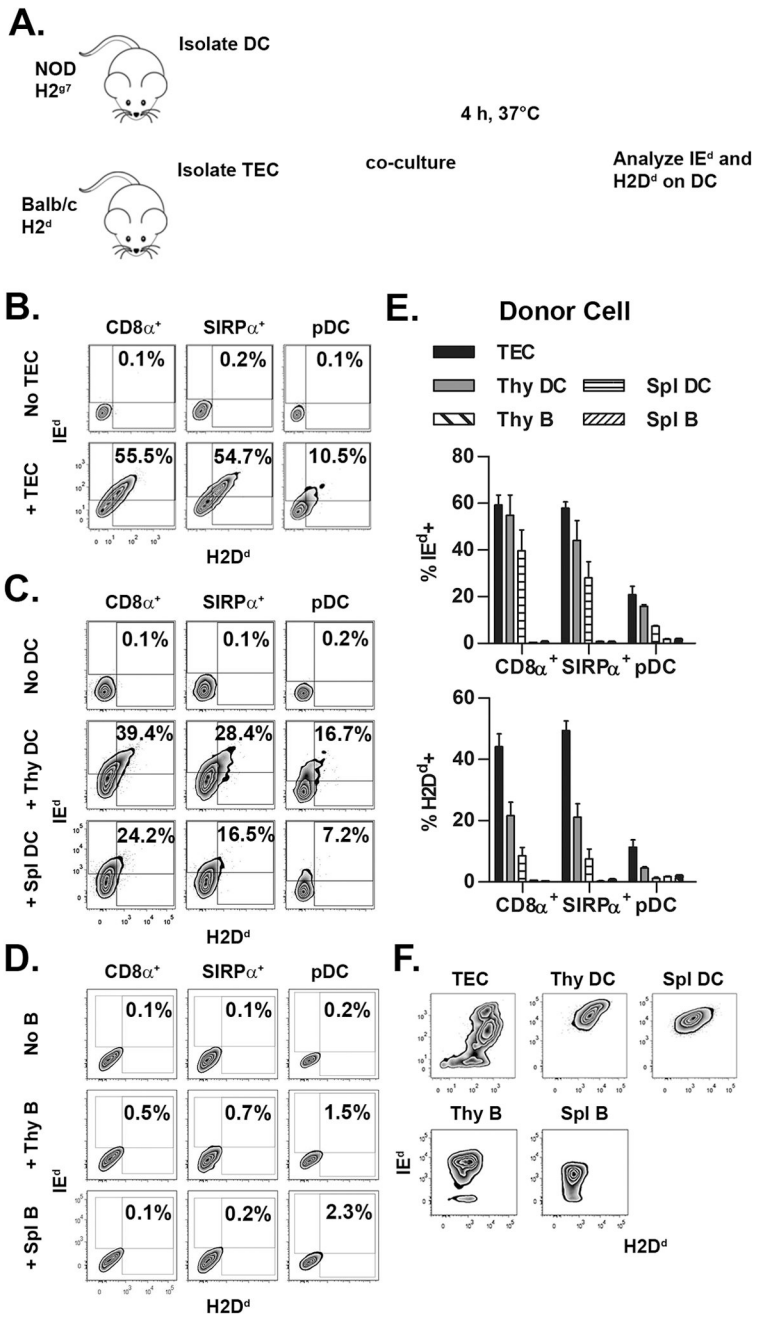


**Figure 1. Thymic DC acquire MHC class I and II from TEC and DC but not B cells**

(A) The design of the *in vitro* intercellular MHC transfer assay. (B–D) Representative flow cytometric plots for $IE^d$ and $H2D^d$ acquisition by NOD thymic DC after co-culture with BALB/c (B) TEC, (C) thymic or splenic DC, and (D) thymic or splenic B cells. All cells were cultured at a 1:2 donor cell to DC ratio. (E) Frequency of $IE^{d+}$ and $H2D^{d+}$ thymic DC after co-culture with the different donor cells. (F) $IE^d$ and $H2D^d$ staining on the different BALB/c donor cell populations. Data is representative of 2–3 experiments.

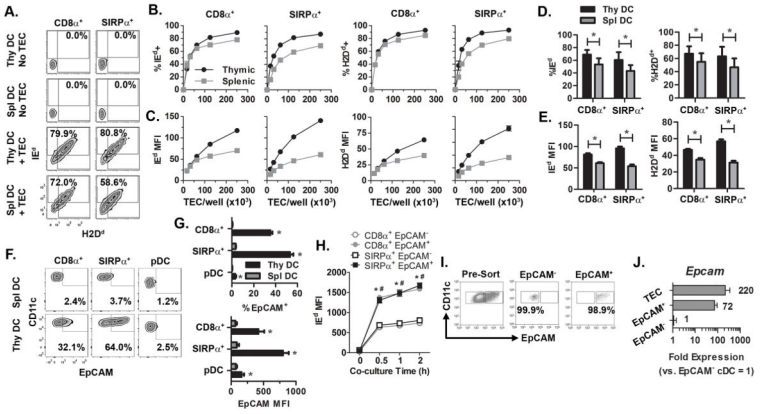

**Figure 2. Thymic versus splenic DC acquire MHC more efficiently, which correlates with DC expression of EpCAM**

(A) Representative flow cytometric plots of $IE^d$ and $H2D^d$ staining of NOD thymic and splenic DC co-cultured with BALB/c TEC at a ratio of 1:2. (B) The frequency of $IE^{d+}$ and $H2D^{d+}$ and (C) MFI of $IE^d$ and $H2D^d$ staining of NOD thymic and splenic DC ($250 \times 10^3$/well) after co-culture with varying numbers of BALB/c TEC from a representative experiment. (D,E) Data depicting the frequency (D) or MFI (E) pooled from2 separate experiments examining the 1:2 cell ratio. *, *P< 0.05,* Student's paired t-test. (F,G) Representative flow cytometric plots, and the frequency of $EpCAM^+$ cells and MFI of EpCAM staining for thymic and splenic DC subsets. Data is the average of 3 mice; *, *P< 0.05,* Student's paired t-test. (H) NOD thymic DC were co-cultured with BALB/c TEC as in Fig. 1 and the frequency of $IE^{d+}$ $CD8\alpha^+$ and $SIRP\alpha^+$ DC determined as a function of time and EpCAM expression. Data is representative of 2 independent experiments. */#, *P< 0.05,* 2-way ANNOVA test. **$CD8\alpha^+$ DC, #$SIRP\alpha^+$ DC.* (I) Representative pre-sort and post-sort analysis of $EpCAM^-$ and $EpCAM^+$ cDC used for RT-qPCR analysis of *Epcam* mRNA. Cells were gated on Live/$CD45^+$/$CD11c^{hi}$. (J) Relative expression of *Epcam* by thymic DC (normalized to $EpCAM^-$ cDC =1). Data are pooled from 3 independent experiments. All error bars represent SEM.

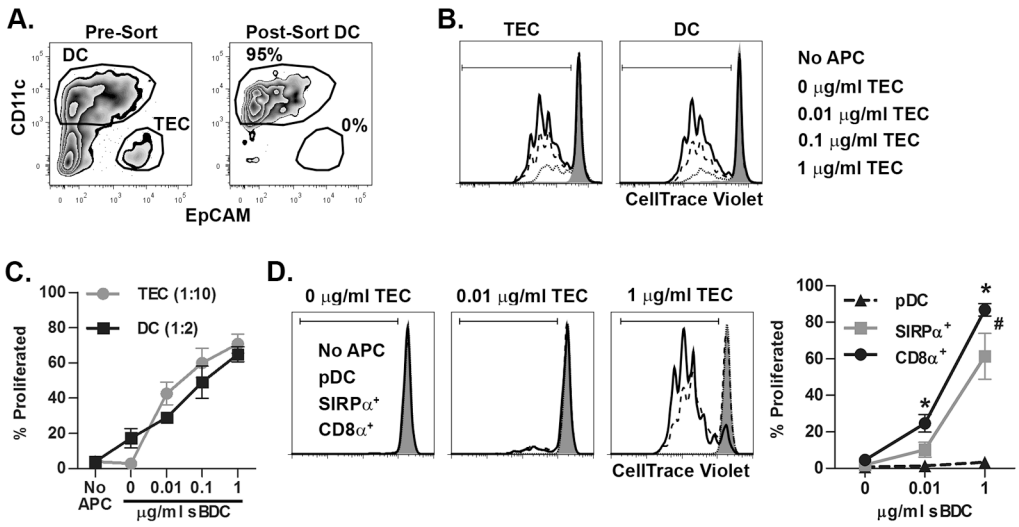


**Figure 3. A hierarchy exists among cross-dressed thymic DC for T cell stimulation**

(A) Representative flow cytometric analysis (gated on live cells) of pre- and post-FACS sorted BALB/c thymic DC ($CD11c^+$ $CD45.2^+$) after 4 h culture with peptide-pulsed NOD TEC ($CD45.1^+$) at a ratio of 1:1. (B) Proliferation of CTV-labeled BDC2.5 $CD4^+$ T cells stimulated by FACS-sorted thymic DC and TEC. Plots were gated on Live/$Thy1.2^+$/$CD4^+$ cells. (C) The average of 3 independent experiments assessing proliferation of CTV-labeled BDC2.5 $CD4^+$ T cells as in (B); ± SEM percent proliferated. (D) Individual BALB/c thymic DC subsets were sorted after the 4 h co-culture with NOD TEC previously pulsed with titrated concentrations of sBDC, and proliferation of CTV labeled BDC2.5 $CD4^+$ T cells measured. Representative and pooled data from 3 independent experiments are shown ± SEM. **/#, P< 0.05,* Student's paired t-test; **$CD8a^+$ DC versus pDC, #$SIRPa^+$ DC versus pDC.*

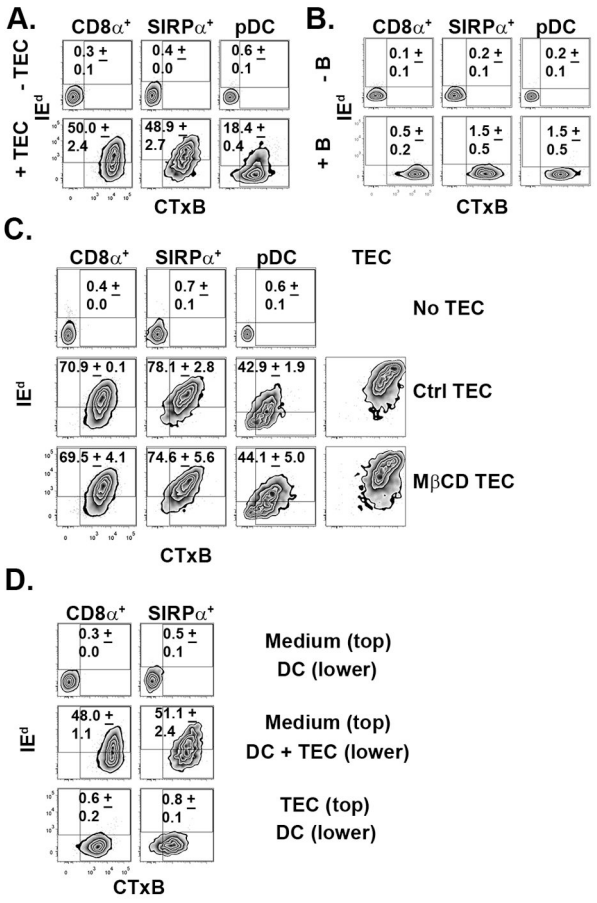


**Figure 4. DC acquisition of TEC MHC class II does not require TEC lipid raft integrity and is cell contact-dependent**

(A,B) NOD thymic DC were purified and co-cultured with CTxB-labeled (A) TEC (1:2 TEC:DC) or (B) splenic B cells (1:1 B:DC) from BALB/c mice, and DC acquisition of $IE^d$ and CTxB assessed via flow cytometry. Data are representative of 3 experiments. (C) Isolated BALB/c TEC were treated with 10 mM MβCD and then co-cultured with NOD thymic DC as in (A). Data are representative of 2 experiments. (D) $IE^d$ and CTxB acquisition by NOD thymic DC cultured with CTxB-labeled BALB/c TEC at a 2:1 ratio in a 0.4 μm TransWell. Data are representative of 2–3 experiments. All numbers within plots indicate frequency of $IE^{d+}$ ± SEM.

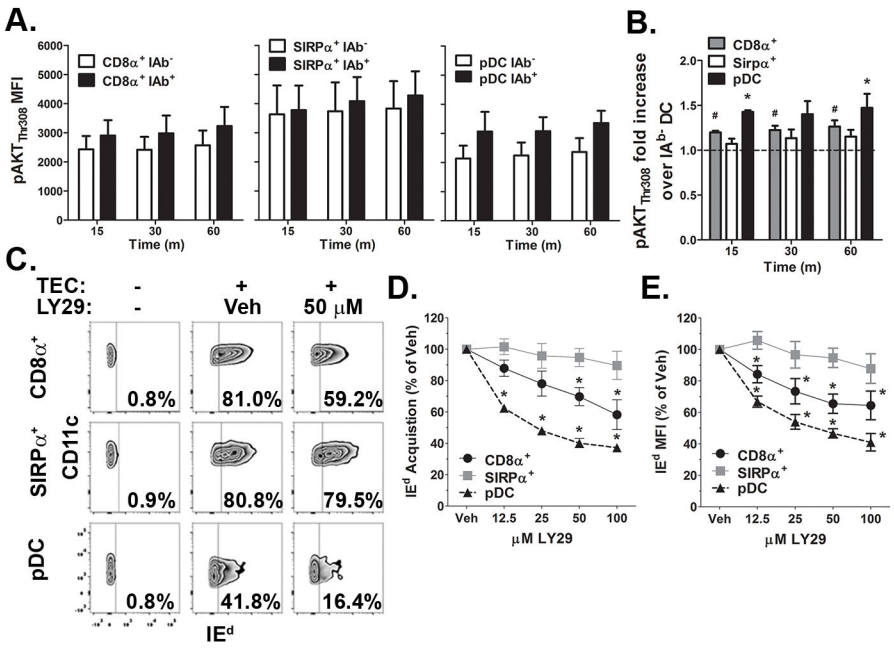


**Figure 5. A thymic DC subset-specific role for PI3K in MHC class II acquisition**

(A) Purified NOD thymic DC were co-cultured with B6 TEC (1:2 TEC:DC) for the indicated time point then fixed. The relative level of $pAKT_{Thr308}$ was determined by flow cytometry on the respective NOD thymic DC that either did not ($IA^{b-}$) or did ($IA^{b+}$) acquire TEC MHC. (B) The fold increase in $pAKT_{Thr308}$ levels in NOD DC was determined by examining the respective MFI on $IA^{b+}$ DC versus $IA^{b-}$ DC at the indicated time points. Data ± SEM are the result of 3 independent experiments. *#/*, P< 0.05,* Student's paired t-test for $CD8\alpha^+$ and pDC respectively. (C) Representative data of purified NOD thymic DC were pre-treated with a titrated concentration of PI3K inhibitor LY29 or DMSO Vehicle (Veh) for 30–60 min prior to and during their co-culture with BALB/c TEC (1:2 TEC:DC) for 2–3 h, and then DC acquisition of $IE^d$ measured via flow cytometry. All numbers within plots indicate percent $IE^{d+}$ for the indicated DC subset. (D) The relative $IE^d$ acquisition efficiency of the respective NOD thymic DC subsets, setting the percent of Vehicle $IE^{d+}$ DC as 100% for each experiment. (E) The relative level of $IE^d$ acquired following LY29 treatment, setting the Vehicle DC $IE^d$ MFI as 100% for each experiment. (C–E) Means ± SEM are pooled from at least 4 experiments for each LY29 concentration. **, P< 0.05,* Student's paired t-test.